Hydro-morphometric parameters controlling travel distance of pebbles and cobbles in three gravel bed streams

Louis Gilet, Frédéric Gob, E Gautier, Geoffrey Houbrechts, Clément Virmoux, Nathalie Thommeret

Hydro-morphometric parameters controlling travel distance of pebbles and cobbles in three gravel bed streams

Louis Gilet*[a], Frédéric Gob[a], Emmanuèle Gautier*[a], Geoffrey Houbrechts[b]., Clément Virmoux[a] and Nathalie Thommeret[c]

[a] Université Panthéon-Sorbonne (Paris 1), Laboratoire de Géographie Physique, CNRS UMR8591, 1 Place Aristide Briand, FR 92195 Meudon cedex, France

*Corresponding author. E-mail address: Louis.GILET@lgp.cnrs.fr

[b] University of Liège, Department of Geography, Hydrography and Fluvial Geomorphology Research Centre, B-4000 Sart-Tilman, Belgium

[c] Laboratoire Geomatique et Foncier, CNAM-ESGT, 1 Boulevard Pythagore, 72000 Le Mans, France

Abstract

This study investigates the parameters controlling bedload distances in several gravel-bed rivers of a medium mountain (Morvan, France). Using PIT tags introduced into pebbles and cobbles, an examination of the relationship between several hydro-morphometric variables and travel distance was first undertaken with bivariate analysis. Bedload distances of our 6 study sites show important differences and this discrepancy cannot fully be understood considering only the stream power for the peak discharge, especially in multi-peak surveys such as ours. Stream impulse, a variable combining flow intensity and flow competence duration, has a stronger correlation with bedload distances. The analysis also indicates a varying influence of relative grain size, relative flow depth, bed slope and width/depth ratio. Among all these parameters, in order of importance, the relative grain size, the slope, and the stream impulse, emerge as the most significant explanatory variables from a multivariate analysis. The role of the relative grain size on bedload transport underlines the importance of grain size sorting and microtopography in plane-bed rivers. The influence of the slope is ambivalent: favoring bedload distances under certain circumstances and lowering them under others. The direction of the influence of the slope seems to depend on its combination with other morpho-sedimentary or hydraulical parameters. Finally, we propose a single equation for bedload distance prediction that predicts travel distance rather well.

Key words

Bedload travel distance; stream impulse; relative grain size; bed slope; gravel-bed rivers; PIT tags

1. Introduction

Bedload travel distance and derived bedload velocity are key features of sediment transport and channel form dynamics. Indeed, bedload velocity controls the rhythm of bar migration (Jaeggi, 1987), pool-bar sequences (Pryce and Ashmore, 2003a, b), sediment wave propagation (Madej and Osaki, 1996; Sutherland *et al.*, 2002) and gravel dispersion (Haschenburger, 2011). Bedload distance and velocity are also used for the calculation of bedload discharge (Laronne *et al.*, 1992; Haschenburger and Church, 1998; Liébault and Laronne, 2008; Houbrechts *et al.,* 2012; 2015; Dell'Agnese *et al.,* 2015; Mao *et al*., 2017a). However, among the very large amount of papers that discuss bedload transport, few focus on travel distance and a lot remains to be done to truly understand the parameters that influence bedload distances and transport velocity.

Particle size is of course a fundamental component to consider when studying sediment transport, for entrainment conditions as well as for displacement length (Robert, 2003). Most of the studies using tracing techniques show that smaller particles tend to cover larger displacements than coarser fractions of the tracers (Hassan *et al.*, 1991; Church and Hassan, 1992. Lenzi, 2004; Scheingross *et al.*, 2013; Schneider *et al.*, 2014). Ferguson and Wathen (1998) emphasized, however, that the influence of the grain size on travel distances (inverse correlation) was more significant for the coarsest fractions of the riverbed substrate. Wilcock (1997) and Lenzi (2004) observed in their studies that displacement length was dependent on the particle size only for coarser sediment moving under partial transport conditions. It was independent of the grain size for smaller, fully mobile grain size fractions. On their side, Church and Hassan (1992) found that the inverse correlation between travel distance and particle size was less obvious for smaller grain-size fractions because they were more frequently and more efficiently trapped within substrate arrangements (buried, locked or constrained within an imbricated structure).

When reviewing the literature, it also appears that the time scale is key when analyzing the relationship between travel distance and grain size. Phillips and Jerolmack (2014) observe a solid inverse correlation between distance and grain size for cumulated displacement length after many hydrological events, whereas the same inverse correlation is weak for the individual flood scale. A poor correlation between grain size and virtual velocity of tagged particles is also observed by Mao *et al*. (2017b) on a short time

scale study. Beyond the grain size factor, bedload propagation rates tend to slow down with time (Ferguson *et al.*, 2002), with vertical mixing and progressive burial of the gravel greatly contributing to its slowdown. This is obviously strongly connected to the magnitude and frequency of flood events (Houbrechts *et al.*, 2015). But storage of gravel in less active and lower energy zones such as point bars, plunge pools and logjams may also moderate the particle displacement (Pyrce and Ashmore, 2005; Houbrechts *et al.*, 2015).

Some studies evaluate the relationship between bedload displacement length and hydrological, hydraulic and morphological parameters that are known to affect or reflect rivers' energy, flow resistance and/or particle resistance to entrainment (Church and Hassan, 1992; Hassan and Church, 1992; Lenzi, 2004; Liébault and Clement, 2007; Lamarre and Roy, 2008; Milan, 2013; Phillips and Jerolmack, 2014; Houbrecht *et al.* 2015; Papangelakis and Hassan, 2016; Klösch and Habersack, 2018). Most of these authors analyze their displacement results in relation to the excess energy above threshold conditions (number of mobilizing floods, competent flow duration, discharge, velocity, specific stream power, shear stress, *etc*.) but such a relationship is still not yet clearly established (Hassan and Bradley, 2017).

This study explores the hydrological and morphological parameters that control the bedload travel distances in three French gravel-bed rivers. In the medium-sized Morvan mountain (central France), our research investigates the role of relative grain size, bed slope, relative flow depth, width/depth ratio, energy magnitude and flow duration on travel distance on plane-bed rivers. To do so, bedload transport was studied on six study sites among three different rivers, all located in the same regional morpho-climatic context. The influence of specific hydro-morphometric characteristics on bedload transport processes at-a-site scale is explored. For every site, we undertook a two-steps analysis: (i) simple bivariate analysis in order to test the influence of the control parameters on the bedload distance; followed by (ii) a multivariate analysis allowing a single relationship for travel distance prediction to be proposed for all of our studied rivers.

2. Study sites

The Morvan massif is a hercynian medium mountain located in the southeast of the Seine catchment (central France) where maximum relief elevation reaches 902 m. (Fig. 1A-B). Its substratum is mainly granitic and gneissic rocks and its climate is temperate oceanic with pluviometry influenced by the orography. The mean annual precipitation in the region is about 900 mm. Combined with the imperviousness of the substratum, this has led to the formation of a channel network featuring a high drainage density.

Six river reaches of three gravel-bed rivers of this region were studied: three on the Yonne river (between 388 and 343 m elevation and, 71 and 83 km^2 for the drainage area), two on the Cure river (between 445 and 295 m elevation, and 160.5 and 234 km^2) and one on the Chalaux river (approximately 395 m elevation, and 69 km^2) (Fig. 1B). They may be considered as medium energy streams with specific stream power for the bankfull discharge fluctuating between 45 and 167 W/m^2 for slopes ranging from 0.0056 m/m to 0.015 m/m (Table 1). The order of the grain size distribution of the bed corresponds rather well to that of the slope values (Table 1). The bed D_{50} and D_{84} range respectively between 0.074 and 0.265 m and 0.105 and 0.699 m, indicating riverbeds dominated by cobbles or small boulders (Table 1 and Fig. 2). With the exception of site S3, our study sites are rather homogeneous and present morphologies that could be qualified as plane-bed. On S3, the grain size distribution is wider and the bed morphology tends to resemble either a light step-pool system or a transverse ribs system (Fig. 2B). Finally, it should be pointed out that the hydrological regimes of some of our study sites are note quite natural as the hydrological regimes are regulated by the releases of a large dam upstream of the Cure river (Settons dam, built in 1858) and by two smaller ones on the Yonne River (Pierre Glissotte and Moulin Blondelot dams, built in the mid-1920s) (Fig. 1B).

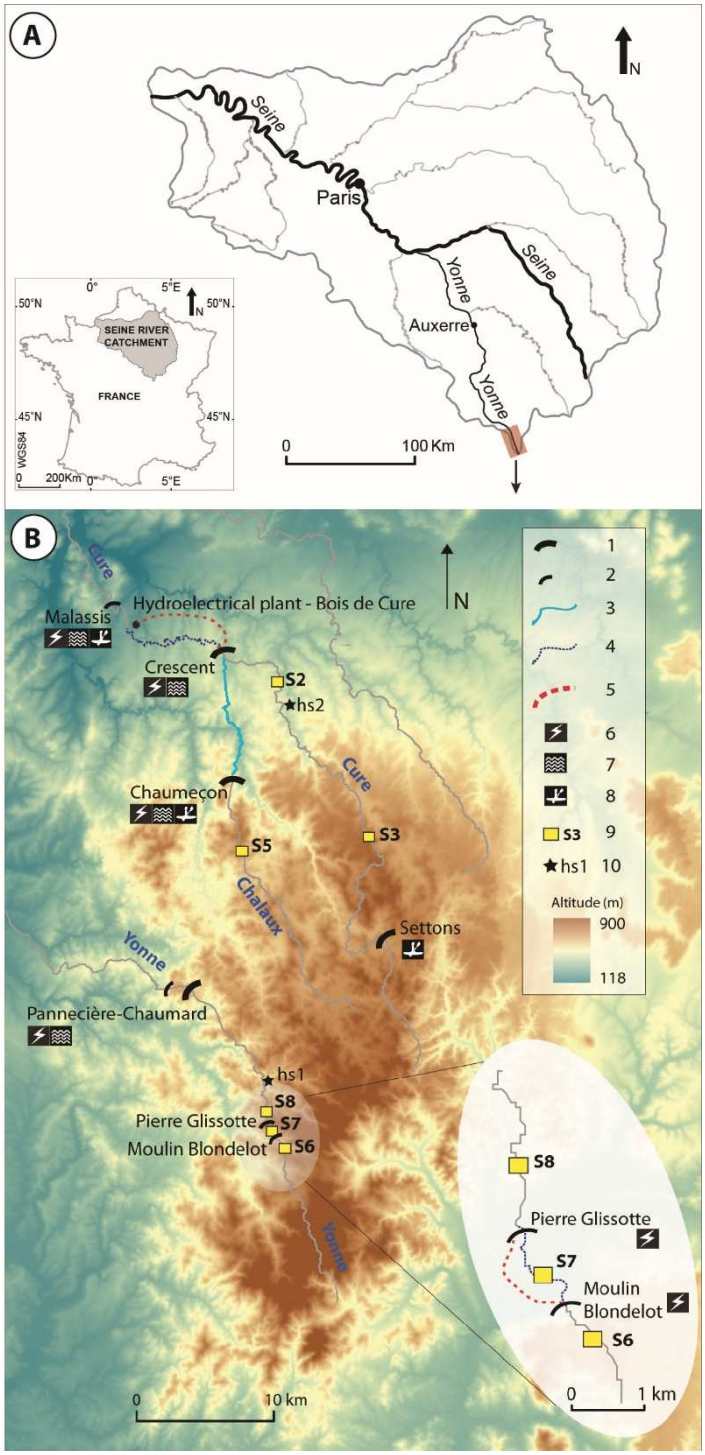

Fig. 1. Locations maps: A) The Morvan massif in the Seine river catchment, B) The study sites on the Yonne and Cure rivers.

1. Large dams (> 15 m); 2. Medium size dams (< 10 m); 3. Regular water-releases; 4. By-passed reach; 5. By-passed canal; Dam function: 6. Hydroelectricity; 7. Flood control; 8. Nautical sports; 9. Study site; 10. Hydrometric station.

113 **Table 1. Characteristics of the study sites**
114

Site number and river	S2 Cure	S3 Cure	S5 Chalaux	S6 Yonne	S7 Yonne	S8 Yonne
Catchment area (km^2)	234	160.5	69	71	74,5	83
Mean annual discharge (m^3/s)	4.76	3.51	1.65	1.84	1.93*	2.15
Bankfull discharge (m^3/s)	20.5	16	6.2	6	5.5	9.5
Specific stream power for bankfull discharge (W/m^2)	78	166.7	48	45.2	77.1	67.7
Bankfull width (m)	18.05	14.12	7.1	9.5	10.5	11.7
Bed slope (m/m)	0.007	0.015	0.0056	0.0073	0.015	0.0085
D_{50} (m)	0.133	0.265	0.080	0.074	0.108	0.083
D_{84} (m)	0.224	0.699	0.142	0.105	0.247	0.175
D_{16} (m)	0.051	0.041	0.023	0.034	0.038	0.037
D_{84}/D_{16} (sorting index)	4.41	17.17	6.17	3.09	6.50	4.69

115
116 * Reconstructed natural flow, if there was not a diversion of the discharge from the upstream Moulin Blondelot
117 dam.
118

119

A-S2 Cure

B-S3 Cure

C-S5 Chalaux

D-S6 Yonne

E-S7 Yonne

F-S8 Yonne

Fig 2. Photographs of the study sites during low or medium flows.

125 The Settons dam was built in 1858 in order to float wood logs. It allowed artificial floods to increase the
126 river's capacity to transport logs that were injected from the river banks at the same time. It is 19 m
127 high and 267 m wide and has a reservoir of 22.7 Mm^3. It is located about 17 km and 31 km respectively
128 upstream of the S3 and S2 study sites. Nowadays, its only function consists of enabling the practice of
129 nautical sports about 30 days/year thanks to water releases. These water releases are mainly operated in
130 spring and autumn, in order to reach a 5 m^3/s discharge on average, and 7/8 m^3/s very occasionally.
131 Those values correspond to 30 to 50% of the bankfull discharge at the downstream study sites. Also, the
132 Settons dam does not control peak flow significantly, as shown on Fig. 3B. This is why the study sites
133 located downstream (S2 and S3) have been considered as non-influenced in the rest of this paper. This
134 assessment is also true for S8, which was not influenced hydrologically by the Pierre Glissotte dam (Fig.
135 1B) because its reservoir was entirely full of sediment preventing any discharge control (Gilet *et al.,*
136 2018). S8, located 1.3 km downstream, presents therefore the same hydrological regime as the upstream
137 non-influenced site (S6, Fig. 3C). S7 is the only site that should be considered as moderately influenced
138 because it is located in a by-passed reach, 300 m downstream of the Moulin Blondelot dam (Fig. 1B).
139 The maximum by-passed discharge is 2.3 m^3/s (for a bankfull discharge of 5.5 m^3/s), but large floods
140 mainly flow through the by-passed reach as they remain poorly affected by the small size of the reservoir
141 (700 m^3) (Fig. 3D). Finally S5 (Fig. 3A) and S6 (Fig. 3C) are located upstream of the dams (Fig. 1B)
142 and they are thus not hydrologically influenced.

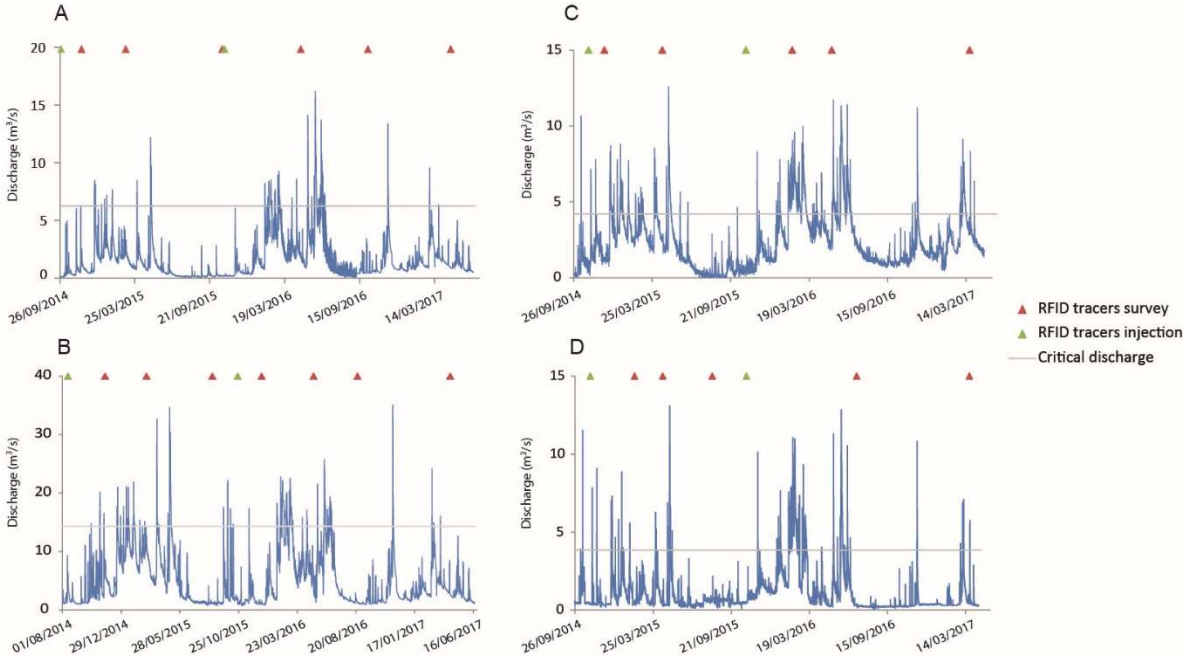

Fig. 3. Discharge recorded on S5 Chalaux (A), S2 Cure (B), S6 (C) and S7 (D) Yonne sites. The vertical and horizontal axes do not have the same scales on the four graphs and the study period on S2 begins earlier. The hydrological regime of S2 is the same as S3, located about 14 km upstream and the hydrological regime of S6 is the same as S8, located about 6 km downstream. The method for the estimation of the critical discharge (for sediment entrainment) is detailed in section 3.1.

3. Methods

3.1 Hydrological monitoring

Two public hydrometric stations provide instantaneous discharges: one located on the Yonne river, 3.3 km downstream of the Pierre Glissotte dam and the other on the Cure river, 28 km downstream of the Settons dam (Fig. 1B). In addition, water sensors (Diver, ©Schlumberger) were installed at the upstream and downstream limits of the 6 study sites. They recorded water level variations every 15 minutes. Coupled with a DEM built from topographical surveys (section 3.2), the upstream and downstream water altitude enabled the reach averaged water depth to be calculated for a given discharge using the HEC-RAS software.

Water levels from water sensors were transformed into discharges with stage-discharge relationships built from our own discharge measurements (electro-magnetic current-meter) and extrapolation from the two public hydrometric stations (using the catchment area-discharge relationship found in Bravard and Petit, 1997). Even though extrapolation always brings uncertainties, comparisons with reference values (extrapolated discharges and our own discharge measurements) gives us a high level of

confidence in our stage-discharge relationships (between 25 and 28 compared values per site; P-value min: 2.2e-16 <, P-value max: 4.8e-14; 0.93 ≤ R^2 ≤ 0.99). The "energy" of the flow was assessed through the calculation of several parameters. Firstly, the specific stream power of the maximum peak discharge that occurred between two surveys of marked particles was calculated. The specific stream power was calculated using Bagnold's (1980) equation:

$$\omega = \rho g Q S / w \quad (1)$$

with ρ the density of water (kg/m^3); g the acceleration due to gravity (m/s^2), Q the discharge (m^3/s), S the slope (m/m) and w the width of the water-surface (m).

In order to consider the entire amount of energy exerted on the bed, the stream power and duration of the peak flows of secondary flood events may also be considered. To do so, integration of flow competence duration was undertaken in diverse contexts over the last thirty years in order to analyze bedload transport and virtual velocity (Hassan *et al.*, 1992; Gintz *et al.*, 1996; Ferguson and Wathen, 1998; Ferguson *et al.*, 2002; Milan, 2013; Phillips and Jerolmack, 2014; Schneider *et al.*, 2014; Houbrechts *et al.*, 2015; Arnaud *et al.*, 2017; Klösch and Habersack, 2018). In this study we proposed a variant of the dimensionless impulse (I_*) introduced by Phillips *et al.* (2013) and Phillips and Jerolmack (2014), and expressed as:

$$I_* = \int_{ts}^{tf} \frac{(U_* - U_{*c})\, dt}{D_{50}}, \qquad U_* > U_c \quad (2)$$

with U_* the shear velocity and U_{*c} the threshold shear velocity for sediment motion, D_{50} the median grain size of the tracers, ts and tf the starting and finishing times of the considered period. According to equation (2), the excess of shear velocity is considered during the delimited period during which sediment transport occurs. These excess values are multiplied by the duration (dt) they are supposed to last and normalized by the D_{50} of the tracers mobilized. In this way, the intensity and duration of the mobilizing flow as well as the particle size is taken into account to examine the river energy consumed for particle transportation. In this study, uncertainties with regard to the calculation of velocities led us

185 to prefer considering specific stream power instead of shear velocity. Consequently, we use an overall
186 time-integrated excess stream power called "stream impulse" (SI expressed in Ws/m^3). It can be written
187 as:

$$SI = \int_{ts}^{tf} \frac{(\omega - \omega_c)\, dt}{D_{50}}, \qquad \omega > \omega_c \tag{3}$$

188 with ω as described in equation (1). In this form SI is rather similar to the excess flow energy expenditure
189 calculated by Haschenburger (2013) and Schneider *et al.* (2014) that reflects the same idea of calculating
190 a time-integrated excess stream power (Hassan and Bradley, 2017). Mao *et al*. (2017b) also show the
191 importance of considering the whole flow series in order to underline the influence of high antecedent
192 flows on incipient motion of sediments and on their virtual velocity.

193 The slope and width needed for the calculation of stream power are both known from topographical
194 surveys: the former corresponds to the reach averaged bed slope and the latter to the reach averaged
195 bankfull width. Critical stream power is calculated from the critical discharge. This is a key parameter
196 as it conditions the whole calculation of excess energy consumed for particle displacement. Incipient
197 motion may be approached empirically using PIT tags and a mobile antenna, but this requires multiple
198 surveys after single low to moderate peak flows. Considering the aims of this study, we have chosen to
199 focus instead on longer time series that include several moderate and high peak flows. Consequently,
200 the lowest mobilizing peak discharge (Q_{lmp}) we may use to determine critical conditions remains for
201 some study sites rather high and the distances covered by the tracers after this peak are relatively long.
202 When compared to the bankfull discharge (Q_{bf}), Q_{lmp} fluctuates between 0.83*Q_{bf} and 1.15 Q_{bf} on our 6
203 study sites for a wide grain size of tagged particles including the large ones (following the study sites,
204 between D_2 and D_6 of the tracers' distribution for the finest mobilized grains, to D_{86} and D_{96} for the
205 coarsest ones). The literature shows that these values are very likely excessive and rather indicates that
206 critical discharges range between 0.25 and 0.8 Q_{bf} (Andrews and Nankervis, 1995; Bravard and Petit,
207 1997; Moog and Whiting, 1998; Pitlick and Cress, 2000; Assani and Petit, 2004; Houbrechts *et al*., 2006,
208 2015, Papangelakis, 2013; Phillips, 2015). Only Métivier *et al.* (2017) and Pfeiffer *et al.* (2017) found

incipient motion close to bankfull conditions. Pfeiffer *et al.* (2017) demonstrated still that τ_{*c} was about 2.35 times lower in the West coast rivers (USA) because of surface armoring. Petit *et al.* (2005) gave several examples of bedload mobilization around 0.7 Q_{bf} in gravel bed streams similar in size, slope and substrate to those of the Morvan. Accordingly, we chose to consider a unique theoretical critical discharge of 0.7 Q_{bf}. This choice was also guided by a few direct additional observations made during gauging campaigns of several of our sites indicating that the bed material began to move for discharges ranging from 0.5 to 0.7 Q_{bf}. Although the critical discharge may not equate exactly to 0.7 Q_{bf} for all of our sites, this approach enables a consistency of the error between the sites.

3.2 Morphological data and grain size distribution

Longitudinal profiles and the cross sectional geometry of the study sites were surveyed with a Trimble total station S6. At least 13 cross sections spaced by 1.5 times the bankfull width were made on each site. These topographical surveys were then used to calculate the bed slope and build a DEM on GIS (Arcgis software), which was then loaded into HEC-RAS software (section 3.1). The grain size distribution of the riverbed was determined using Wolman's surface sampling method (1954). We tried to respect a sampling step equating to twice the b-axis of the largest particle of the sampled unit (Lejot, 2008; Belliard *et al.*, 2009). Three sub-reaches were delimited along the study reach as a function of their apparent geomorphological homogeneity (bankfull width and depth, grain size range, substrate arrangement) even if geomorphological variations within the same reach were generally very limited. At least 100 particles per sub-reach were sampled and measured, resulting in a minimum of 300 particles per site.

3.3 Bedload transport monitoring

Bedload transport was studied with Radio Frequency Identification (RFID) technology. Individual particles were tagged with a Passive Integrated Transponder (PIT) that can be identified by a unique number thanks to the RFID technology. This is now commonly used for bedload transport studies (Lamarre *et al.*, 2005; Rollet *et al.*, 2008; Liébault *et al.*, 2012; Bradley and Tucker, 2012; Chapuis *et al.*, 2014; Phillips and Jerolmack, 2014; Houbrecht *et al.*, 2015; Dépret *et al.*, 2017). The technique presents numerous advantages and a series of limits well described by Piegay *et al.* (2016). Among the

benefits of the technique, are the fact that the tracers are not disturbed between detections, as well as the relatively low cost and the long lifetime of the tag. With regard to limitations, one may mention that this is a time consuming method, there is an initial modification of the bed structure when sampling the bed, and the PIT tags cannot be detected when buried under a range of sediment depth values varying between 20 cm (Houbrechts, 2012), 45 cm (Chapuis *et al*., 2014) and 70-89 cm (Arnaud *et al*., 2015), for the "small" circular antennas that we used. During our field surveys, in the few instances when it was possible to test this detection range, it appeared that tracers were hard to detect beyond 25 cm of burial depth.

In this study, 50 tagged particles (tracers) were first injected at each site between August and October 2014 (Table 2). At the study sites with active bedload transport, some initial tracers may rapidly have been able to go farther than the prospected area. 25 additional tracers were then injected in October 2015. The particles to tag were selected in the riverbed using the Wolman coarse grain sampling method (1954). However, the tracers' size range does not completely follow grain size distribution of the bed because the tags we used were 32 or 23 mm long. Consequently, no particle with a b-axis under 20 mm was tagged. Also, for logistical reasons we were not able to tag more than few particles per site with a b-axis above 130 mm. This led to a slight discrepancy between the D_{50} injected and the D_{50} of the bed, that is accentuated with the D_{84} percentile (Table 2). On sites with the largest grain size, this could have led to a slight overestimation of the mean distance travelled by the tracers over the potential mean distance travelled by the "unmonitored" bedload. This possible overestimation of the travel distance is discussed in section 5.5.

Tracers were injected along the cross sections at an interval of 1.25 m. Each cross section was separated by at least 2 m. Surveys of the tracers' positions were undertaken between November 2014 and April 2017 with a round, 0.55 m-diameter antenna. The distances travelled by the marked particles were measured using a flexible ruler (tape measure) unrolled along the bank. Due to the degree of precision of the measurements (antenna radius: 0.5 m), tracers were considered as mobile when they had moved forward at least 0.6 m beyond their previous known position for the first 80 m of the study sites. Beyond 80 m, we considered mobilization if the tracers moved more than 1 m. This increase in error margin is

263 based on the observation that beyond a 75-85 m length, noticeable disparities (from 0.02 m to 0.06 m)
264 in the ruler roll-out between two surveys can appear owing to irregularities along the bank (trees,
265 boulders).

266 Except if mentioned otherwise, the displacements recorded during the first survey after injection are not
267 displayed in the results below. Even if tracers were carefully inserted within the alluvial substrate, by
268 excluding the displacements recorded during the first survey we aim to prevent any "artificial"
269 protrusion effect favoring tracers' mobility (Bright, 2014; Houbrechts *et al*, 2015; Olinde and Johnson,
270 2015).

271 In addition, we paid attention to only compare the monitoring results of tracers obtained with equally
272 good surveying flow conditions: i.e. when the water level and flow strength were low enough to prospect
273 more than 90 % of the reach area (except for the specific S6 site, where a section of the fluvial reach
274 between 120 and 160 m length is permanently hard to access because of water depth and slippery
275 substrate). In the end, except when cumulative distances are discussed in section 4.1, the bedload data
276 presented in this paper come from three surveys realized on each of the Yonne sites (S6, S7, S8), four
277 surveys on the Chalaux (S5) and S3 Cure sites, and five surveys on the S2 Cure site.

278

279

280

281

282

283

284

285

286 **Table 2. Details of the injected PIT tag tracers**
287

Site and river	S2-Cure	S3-Cure	S5-Chalaux	S6-Yonne	S7-Yonne	S8-Yonne
Injection date (50 first tracers)	15/08/14	16/08/14	29/09/14	30/10/14	31/10/14	31/10/14
Last survey date (duration in years)	18/04/17 2.7)	20/04/17 (2.7)	22/04/17 (2.6)	22/03/17 (2.4)	24/03/17 (2.4)	23/04/17 (2.5)
Total number of tracers	75	50	75	75	75	75
D_{50} injected tracers (mm)	63	60	62	58	58	63.5
D_{50} injected tracers / D_{50} riverbed	0.47	0.23	0.78	0.78	0.55	0.76
D_{16} injected tracers / D_{16} riverbed	0.88	0.97	1.86	0.97	1.02	1.13
D_{84} injected tracers / D_{84} riverbed	0.50	0.13	0.68	0.79	0.37	0.55

288

289 ## 4. Results

290 ### 4.1 Relationship between bedload distances and river energy

291 Fig. 4 and Table 3 give a first overview of the cumulative bedload transport observed at each site about
292 2.5 years after the injection of the first tracers. One may first notice a different intensity according to the
293 rivers: the Yonne and the Chalaux appear to be rather dynamic systems (in terms of distance travelled
294 and mobilization rates), while the Cure presents lower bedload transport activity. A distinction may
295 however be made between the S2 Cure site and the S3 Cure site. S2 presents medium transport activity
296 but a mean travel distance close to the S6 Yonne site, while the S3 site shows a noticeably low transport
297 activity. At all of the study sites considered, the mean distance travelled by the tracers varies between
298 24 m to 315 m over about 2.5 years (the cumulative travel distances at S6 are probably underestimated
299 as mobile tracers located in the previously mentioned "hard to survey" sub-reach, between 120 and 160
300 m, are not taken into account). If we exclude S6, the largest particles injected have not been significantly
301 transported (or not transported at all) and sediment sorting has clearly developed on sites S2, S5, S7 and,
302 in a less obvious way, on S8. In Table 3, the D_{50} of the mobilized tracers is close to or slightly under the

303 median size of all detected tracers (i.e. D_{50} tracers, which does not exactly equate to the injected tracers'

304 D_{50} from Table 2) and is therefore still much smaller than the D_{50} of the bed (Table 1).

305

306

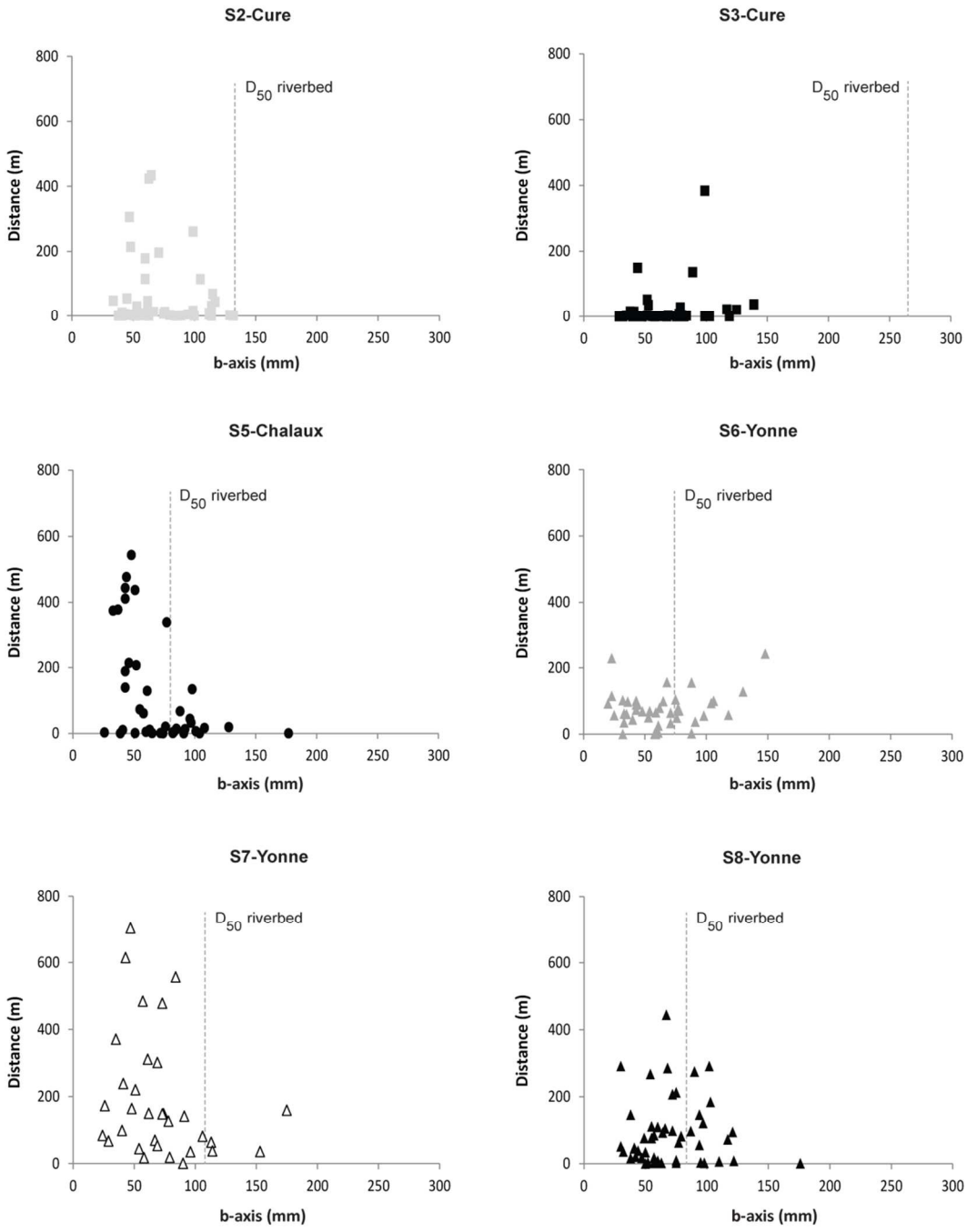

307

308 **Fig. 4. Relationship between cumulative bedload distances and the median diameter of tracers**
309 Distances are based on the results of the last monitoring survey only.

310

311 **Table 3. Cumulative data on bedload transport in Morvan rivers**
312

Site and river	S2-Cure	S3-Cure	S5-Chalaux	S6-Yonne	S7-Yonne	S8-Yonne
Mean distance (m)	67.5	24	141	78	315	123
Di_{max} mobilized (mm)	144	139	128	148	175	122
D_{50} tracers (mm)	62.5	59	73	69.5	61	75
D_{50} mobilized tracers (mm)	63	65.5	58	61	58	68
Mobilization rate	0.69	0.50	0.80	0.91	0.97	0.94

313 Distance values are based on the results of the last monitoring survey only and the mean values include tracers that
314 did not move. The D_{50} tracers represents the median grain size of the detected tracers, including tracers that did
315 not move. D_{50} mobilized tracers include only mobile tracers.

316 **4.1.1 Excess stream power and duration of the competent flow**

317 The excess stream power of the highest peak discharge between two PIT tag surveys is compared in Fig.
318 5 to the mean distances travelled during this same period. Though the data set of our 6 study sites is
319 rather coherent with observations from the literature (Hassan *et al.*, 1992; Gintz *et al.*, 1996; Lenzi,
320 2004; Schneider *et al.*, 2014; Houbrechts *et al.*, 2015), no evident relationships appear and the data
321 presents a large scatter around the literature relationships. This large dispersion of the data first reflects
322 a certain diversity of functioning between the different sites despite the apparent homogeneity of the
323 rivers studied. This suggests that the inner diversity of the sites (slope, channel geometry, roughness and
324 structure of the bed) has to be explored in detail. The Cure river experienced much shorter displacement
325 than the other river reaches. Yet S3 is the study site presenting the steepest slope (0,015 m/m), the largest
326 D_{50} (26.5 cm) and the highest D_{84}/D_{16} ratio (17.17) (Table 1). The potential influence of high bed
327 roughness on the displacement of particles should be investigated further.

328

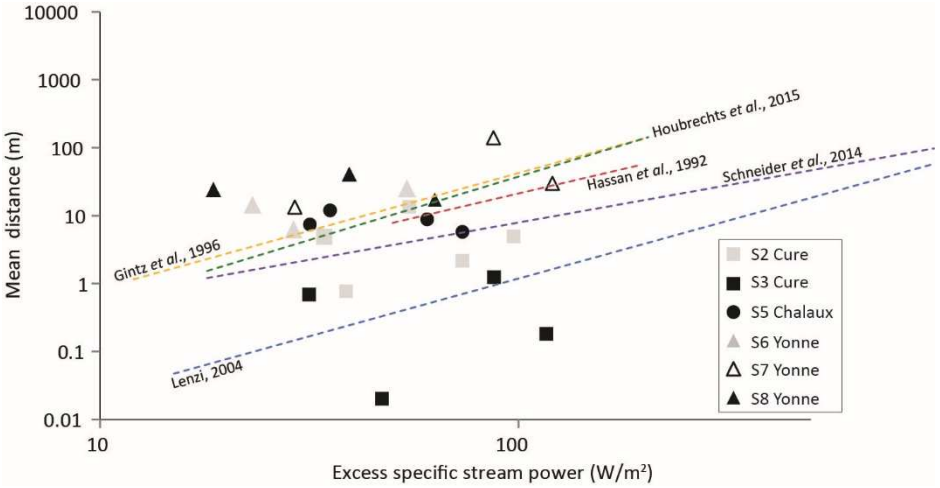

329

330 **Fig. 5. Relationship between the mean inter-survey distance (0 values included) and the maximal**
331 **inter-survey excess specific stream power.**

332 Indeed another notable issue appears from the Fig. 5. There is a very poor relationship between excess
333 stream power and the corresponding mean distance (even within the same site). Indeed if a regression
334 line were plotted for each site, most of the time the surveys involving the most powerful peak flows
335 would never correspond to the longest mean distance travelled. The correlation is even negative in many
336 instances, with travel distance relatively shorter for the largest flood events. The magnitude of the
337 highest flow peak is in our case not sufficient to describe travel distance.

338 **4.1.2 Stream impulse**

339 In order to combine duration and magnitude of the overall flow over the critical threshold, we considered
340 the stream impulse (SI) presented in the Eq. (3). Fig. 6 shows the relationship between SI and the
341 corresponding mean distance. It shows that the use of stream impulse is more adapted for the
342 understanding of our bedload distance data. Indeed, almost all sites show a clearer positive relationship
343 between energy, flow duration and travel distance. Three groups of sites appear now rather clearly. They
344 are mainly based on the differences of distance range for a given stream impulse range and they gather
345 sites with some common morphological features.

346 The first group concerns the most dynamic sites, S7 and S8 on the Yonne river (regression A, $R^2 = 0.78$.
347 P-value= 0.018). The second group gathers the observations of S2, S5 and S6 (regression B, $R^2 = 0.27$,
348 P-value=0.081). The last one confirms what Figs. 5A and B had already shown: despite similar or higher

stream impulse values, the tracers at S3 travel shorter distances than at the other sites (regression C, R^2 = 0.98; P-value=0.01). As already mentioned, S3 is the steepest reach (s = 0.015 m/m) with a stream bed that includes a lot of large cobbles (D_{50} = 26.5 cm). Group A is almost as steep (s > 0.008 m/m) but with smaller particles (D_{50} = 8.3 and 10.8 cm). Meanwhile, group B reaches have lower slopes (s < 0.0075 m/m) but show a wider range of median grain size (7.4 < D_{50} <13.3 cm). This group may be slightly less homogeneous morphologically (e.g. bankfull width, Table 1). On Fig. 6, the dots from group B are also a bit more scattered (S2 especially) and this explains the low coefficient of determination and their statistical non-significance according to P-value calculation.

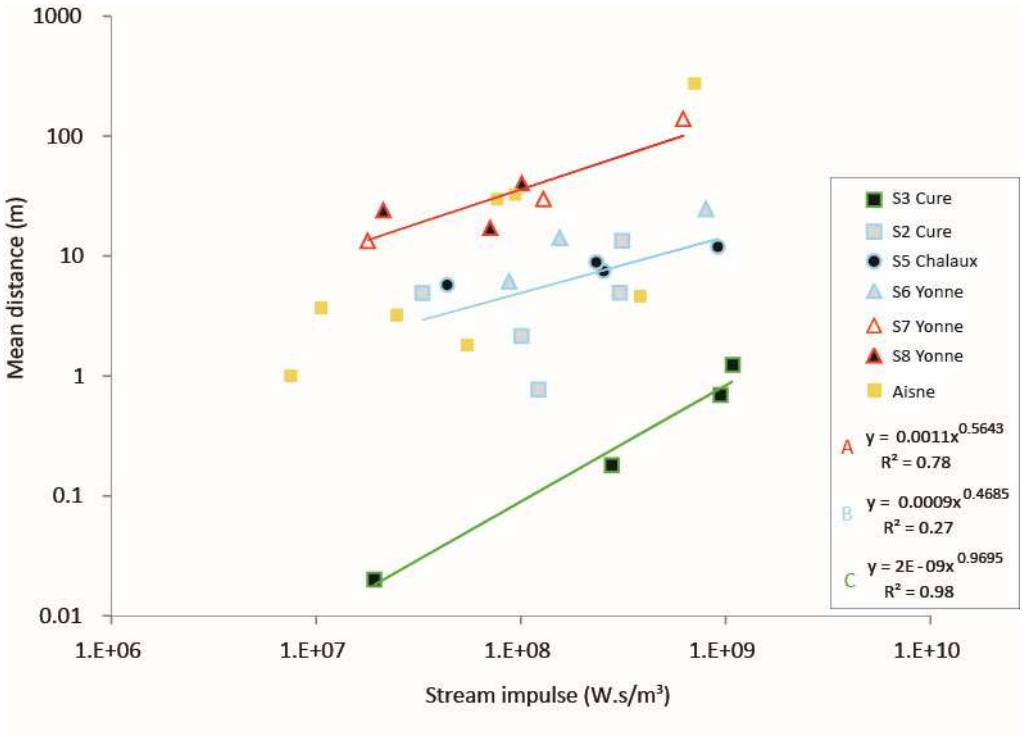

Fig. 6. Relationship between the mean travel distance and the stream impulse (SI). Colored borders of dots and colored curves highlight the three groups (A, B, C) that have been distinguished.

Data used by Houbrechts *et al.* (2015) on the Aisne river were plotted in Fig. 6 for comparison. This river flows in Southern Belgium within a morpho-climatic context quite similar to the Morvan massif. The D_{50} of the bed is 9.2 cm, its slope 0.0053 m/m and its bankfull width 13.57 m, and the critical discharge for particle entrainment represents 55% of the bankfull discharge. The correlation between

365 mean distance and stream impulse is also rather obvious for the Aisne data (R^2 = 0.53; P-value = 0.04).
366 The Aisne scatter plot shows a trend similar to the Morvan's A and B relationships.

367 Despite "time" and "storage processes" as potential complexity factors on the Aisne river (see
368 Discussion section, 5.2), Fig. 6 shows clearly that using the stream impulse (SI) allows the description
369 of the travel mean distance of the tracers to be greatly improved. Nonetheless, the dispersion of the
370 Morvan data remains quite large and, at this stage, the reasons why still have to be clarified.

371 **4.2 Relationship between bedload distances and morpho-hydraulic parameters**

372 The mean travel distances of tracers has been normalized by different morphological and hydraulic
373 parameters (Fig. 7A-D) in order to identify the reasons behind the discrepancy observed on Fig. 6. The
374 parameters are: relative grain size corresponding to the $D_{50\ tracers}/D_{50\ bed}$ ratio (A), where the first term is
375 the D_{50} of the tracers whose displacement distance is known, immobile tracers included; bed channel
376 slope (B); relative flow depth (C), given by the ratio between the reach averaged water depth for the
377 peak discharge of the inter-survey period and the D_{84} of the bed; and reach averaged width/depth ratio
378 for the peak discharge of the inter-survey period (D).

379 In Fig. 7A-D, 3 groups of data can be distinguished again and they are globally the same groups
380 described in Fig. 6. However the gap between the relationships fluctuates following the parameter used
381 for normalization, giving a clearer idea of what and how morpho-hydraulic features may influence
382 bedload travel distance on each study site.

383 The relative grain size is likely to influence S3 travel distances, as can be seen from the normalization
384 in Fig. 7A, which brings S3 closer to the other sites (compared to Fig. 6). The relative grain size of the
385 tracers on this site is by far the lowest (Table 4) and a hiding effect may then contribute to explain the
386 low recorded distances. Compared to Fig. 6, S7 and S8 data are closer to S3 data on Fig. 7A because
387 their tracers have on average a relative grain size that is much higher than the relative size of S3 tracers
388 (Table 4). In S7 and S8, boulders are present but they are less numerous and they are smaller than on
389 S3. S7 and S8's riverbeds are also much better sorted in terms of grain size than S3's riverbed, where a
390 deficit of medium sized particles can be observed (Table 1). The relative grain size may also contribute

391 to the relative scattering of the Group B data for a comparable stream impulse, observed on Fig. 7 as
392 well as on Fig. 6. S5 and S6 present the highest values whereas S2's mean relative grain size is much
393 lower (Table 4).

394 The different groups of study sites present a more unclear relationship with the bed slope (Fig. 7B). The
395 higher bed slope of the A and C groups ($s \geq 0.008$ m/m, Table 4) increases normalized travel distances
396 to a lesser degree than for the sites of the intermediary group (S2, S5 and S6) which have lower slopes
397 ($s \leq 0.0073$ m/m) (Fig. 7B). S7 and S8 data are then closer to these intermediary sites in Fig. 7B, when
398 S3 appears even more isolated. A significant slope is therefore associated with short (group C) and long
399 (group A) bedload travel distances, and a moderate slope corresponds to the group with intermediary
400 bedload distances (B).

401 The relative flow depth on S3 group C is also shown as a parameter that may contribute to the low travel
402 distances, as emphasized by its use for normalization that clearly gets S3 data closer to B group (Fig.
403 7C). The high slope and the presence of boulders on S7 and S8 induces a relative flow depth that is
404 lower than the intermediary B group (except for S2), increasing the disparity between groups A and B
405 (Fig. 7C). Thus, a group of data is showing important bedload displacements despite a low relative flow
406 depth (A) and another shows very short bedload displacements that may be partly explained by a very
407 low relative flow depth (C). In group B, S2 presents a large D_{84} leading to a mean relative flow depth
408 close to S8 and just higher than S7. This is why normalization of mean distances with relative flow depth
409 does not "move" S2 data as far from S7 and S8 as it does for S5 and S6 (Fig. 7C). Indeed, these have
410 the highest relative flow depth values because of lower bed slope, D_{84} and bankfull width values (Table
411 1 and Table 4). This higher relative flow depth, combined with the higher relative grain size and the
412 substrate homogeneity on S6 (Table 1, index sorting), are hydro-morphometric features that may
413 "compensate" the lower bed slope of these sites. This suggests, however, that (increasing) slope as a
414 parameter fostering bedload transport as on S7 and S8 should be considered. The positive or negative
415 effect of the bed slope will be further questioned in section 5.4.

In group B, for S5, bedload mean distances may also be supported by a very low w/d ratio, compared to the other sites (Table 4). This may favor increased bedload travel distance as potentially indicating a higher depth during floods and then a higher shear stress for a given discharge. The normalization with this parameter (Fig. 7D) clearly brings S5 data closer to S7 and S8. Inversely, the Cure sites have the highest w/d ratios because of their larger width (S2), or their low flow depth due to bed slope (S3). This maintains S3 normalized distances beneath the other sites' values and lowers S2 data. These even tend to separate from other data of the B intermediary group (Fig. 7D), underlining once again the link between different morpho-hydraulic parameters and scattered bedload distances within this group itself.

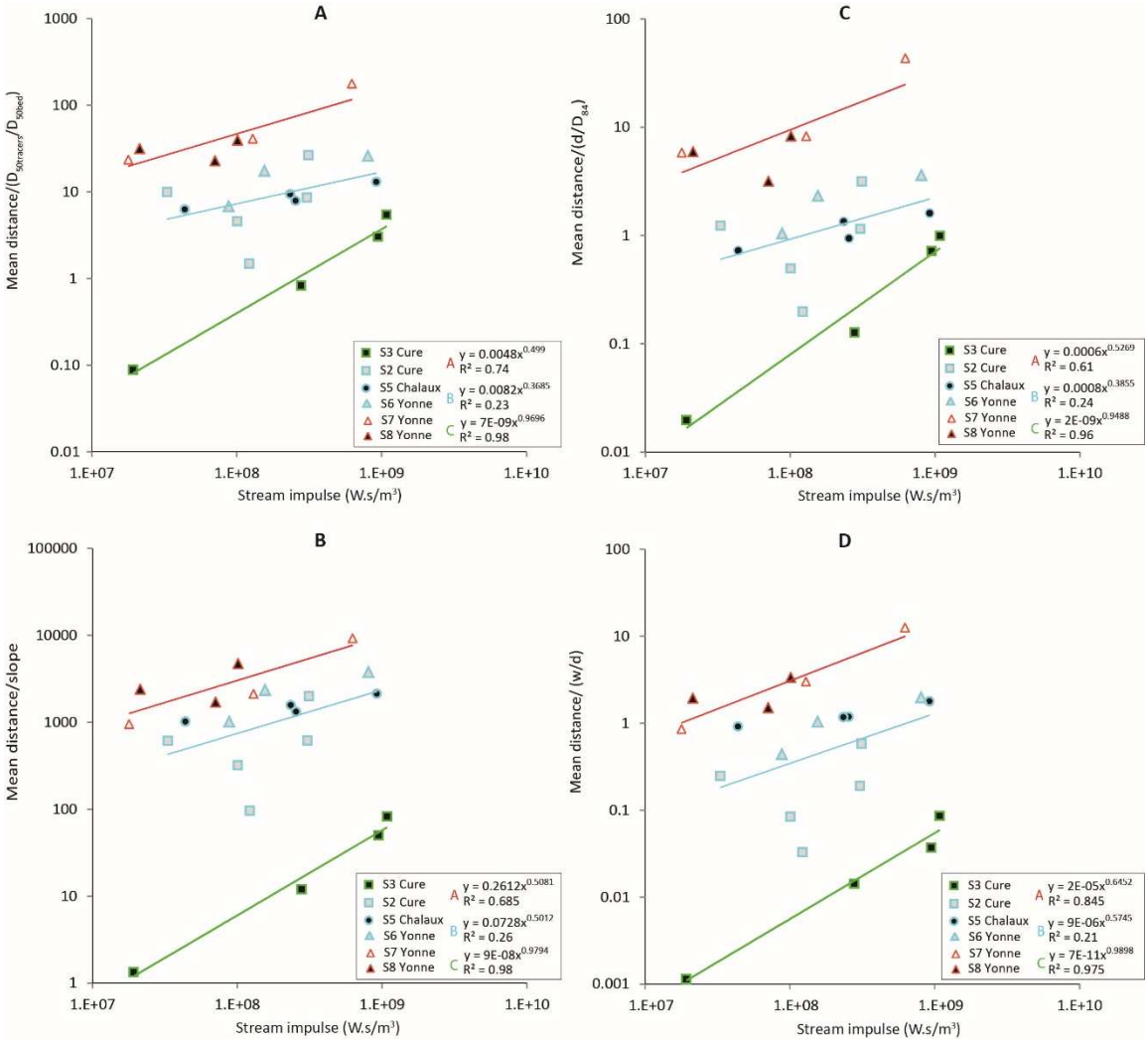

Fig. 7. Relationship between mean travel distance normalized by hydro-morphometric parameters and stream impulse (SI). A) Mean travel distance normalized by relative grain size, B) Mean travel distance normalized by the bed slope, C) Mean travel distance normalized by relative flow depth, D) Mean travel distance normalized by the width/depth ratio. Equations correspond to the best-fit relationship.

Table 4. Mean values of the morpho-hydraulic parameters

Site and river	S2-Cure	S3-Cure	S5-Chalaux	S6-Yonne	S7-Yonne	S8-Yonne
Mean* relative grain size of the tracers	0.51	0.23	0.93	0.88	0.69	0.84
Bed slope (m/m)	0.007	0.015	0.0056	0.0073	0.0015	0.0085
Mean* relative flow depth	4.14	1.14	7.43	6.25	3.03	4.76
Mean* Width/depth ratio	23.5	17.2	6.7	13.3	12.1	11.8

*Corresponding to the mean value of the different RFID surveys or inter-survey periods.

4.3 Stepwise multiple linear regression

Simple bivariate regressions of Fig. 7 allowed parameters that discriminate mean travel distance to be identified. However, in order to quantify the degree of influence of each parameter and propose a single relationship allowing mean distance to be predicted, stepwise multiple linear regression was tested. The five parameters tested were chosen according to the results of the bivariate relationships presented above: stream impulse (SI), relative grain size ($D_{50tracers}/D_{50bed}$), relative flow depth (d/D_{84}), bed channel slope (s) and width/depth ratio (w/d). Only three of them were finally defined as having a significant influence during the analysis (Table 5), allowing the following prediction model to be proposed:

$$\bar{L} = \text{EXP}\,(7.3805 + 0.4069\ \text{LN}\,(\text{SI}) + 3,8896\ \text{LN}\left(\frac{D_{50\ tracers}}{D_{50\ bed}}\right) + 2.3694\ \text{LN}\,(\text{S})) \quad (4)$$

Where $\bar{L}$ is the mean bedload distance, SI the stream impulse, D_{50} tracers is the median grain size of the tracer whose displacement distance is known, immobile tracers included, and S is the bed slope. This model has a quite convincing adjusted coefficient of multiple determination ($R^2 = 0.73$) with a rather good residual standard error of 1.064, P-value <0.001 and F-statistic = 17.43.

Table 5. Results of the stepwise multiple regression

	Std. Error	t value	P-value r(>|t|)	Significance
Intercept	4.8936	1.508	0.14796	**
Log (SI)	0.1804	2.256	0.03606	*
Log ($D_{50tracers}/D_{50bed}$)	0.5771	6.740	1.93e-06	***
Log (s)	0.8055	2.941	0.00838	**

The model provides quite strong predictions for most of our study sites. Once again it is the S3 site on the Cure that diverges most from the other study sites. In this case, our model poorly predicts two S3 surveys with a clear overestimation of the low tracer displacement (Fig. 8). A test was also realized with the Aisne river data (Houbrechts *et al.*, 2015). These were not included in the multiple regression

analysis that enabled to build the Eq. (4). The test tends to validate the model as we obtain predicted distances that genuinely match for all but one of the observed distances (Fig. 8).

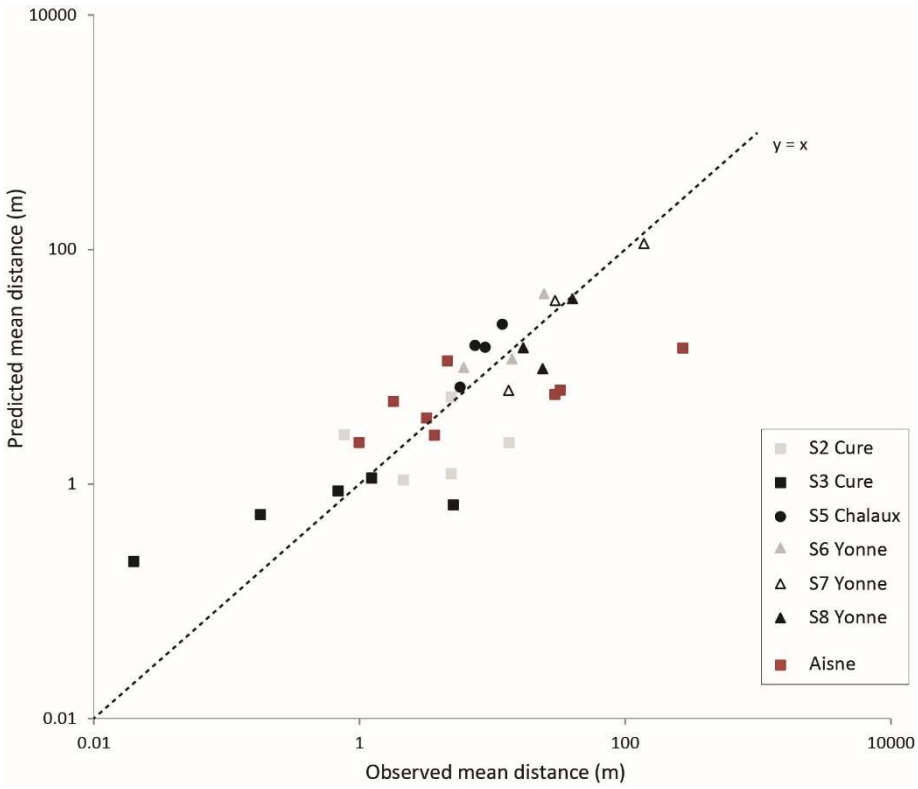

Fig. 8. Comparison between the observed mean distance of tracers and the predicted mean distance from Eq. (4).

When looking at Fig. 8 in more detail, one may notice a slight offset of certain data towards the bottom of the graph (i.e.) indicating an underestimation of the predicted distance. This concerned notably the three largest mean distances observed on the Aisne river. These three largest mean observed distances on which this underestimation applies were also recorded for three of the four inter-survey periods with the highest stream impulse. A possible underestimation of the stream impulse for high flow events is discussed in the section 5.2.

5. Discussion

5.1 Bedload dynamics poorly explained by the commonly used hydraulic parameters

Bedload travel distances recorded on Morvan rivers are very different according to the study sites (Table 3 and Fig. 4). Also, for the same site, the travel distance appear moderately correlated with the higher flood peak (Fig. 5A). The longest displacements are rarely coupled with the greatest excess stream

power. Conversely, in many instances, the largest events correspond to shorter displacements. This is quite counterintuitive and diverges from what the literature has repeatedly shown (Hassan *et al.*, 1992; Gintz *et al.*, 1996; Lenzi, 2004; Schneider *et al.*, 2014; Houbrechts *et al.*, 2015).

Comparisons with the literature may bring precious information but should be used with caution because of the differences in methodology (first peak or maximal peak discharge considered, tracer replacement, number of flood peaks considered) that may lead to very divergent results. Indeed, Fig. 5 shows that our results do not entirely match with data from the literature. Moreover, while the Morvan data has been acquired only in plane-bed channels, the data from the literature presents a dispersion corresponding to results from a wide range of bed morphologies: fr0om other plane-beds (Houbrechts *et al.*, 2015) to riffle-pools (Hassan *et al.*, 1992; Houbrechts *et al.*, 2015) and even step-pools (Gintz *et al.*, 1996; Lenzi, 2004; Schneider *et al.*, 2014).

The high rate of displacement related to a short inter-survey period observed in our data set for two surveys (S7 and S8) is a good example of this methodological question. They present high distances for a relatively low competent flow duration and low excess stream power peak because of the short period we left between the previous surveys (65 days for S7 and 69 days for S8). Long distance traveled may then have been stimulated by tracers not well inserted in the bed structure and by transport mostly operated during the first hours (or the first event) of the competent flow. These elements echo a recent study from Dell'Agnese *et al*. (2015) underlining the influence of different flow competent durations on bedload virtual velocity through the capacity to get closer to the actual virtual velocity.

The weak correlation between bedload displacements and the maximal excess stream power of our data may also be explained by the way the excess stream power is calculated (Fig. 5). Indeed, only the highest peak discharges of the inter-survey periods are considered. Meanwhile, each of these periods encompasses several flood peaks of variable magnitude and duration. This, therefore, should lead to noticeable differences with results from "one-peak survey" studies such as those of Gintz *et al.* (1996) or Houbrechts *et al* (2015). With this in mind, considering only the magnitude of the highest peak is clearly not adequate to describe our bedload displacements. The multi-peak characteristics of our

surveys forced us to explore the role played by the combination of the magnitude of the high flows and their duration, as suggested by Papangelakis and Hassan (2016) amongst others.

5.2 Relevance of the stream impulse in a multi-peak survey

Inspired by the dimensionless impulse developed by Phillips and Jerolmack (2014) and echoing the excess energy expenditure used by Haschenburger (2013) and Schneider *et al*. (2014), the stream impulse (SI) enables the flow competence duration and the overall excess stream power to be integrated.

On Morvan rivers, the bedload mean distance is clearly better correlated with the stream impulse than with the sole magnitude of the largest peak flow, especially when grouping the data according to the riverbed characteristics (Fig. 7). This should, however, be considered with some nuances as some of these relationships are built on a limited number of dots.

The introduction of independent data from the Aisne river, confirms the relevance of using the stream impulse to characterize the flows. However, the Aisne river data also brings forward the potential influence of time and burial phenomenon (Ferguson and Hoey, 2002; Haschenburger, 2011; Houbrecht *et al*., 2015). Indeed, the two lowest dots of the Aisne data on Fig. 6 have been surveyed 5.5 and 6.3 years after the initial injection of tracers, when the other monitoring surveys occurred within 3.3 years following the injection, and following a 10-year flood event. This indicates that major events as well as simple elapsed time since injection have probably contributed to vertical mixing and burial of a part of the tracers, making them less easy to entrain and thus reducing the distance travelled. This leads us to emphasize that our study has been realized for a limited duration (about 2.5 years) and to question if the good correlation between travel distance and stream impulse would be maintained on a longer time scale.

The relationship resulting from the stepwise multiple regression (Eq. (4)) also confirms the interest in considering stream impulse to predict the mean distance travelled by the particles. The calculation of the mean distances on the Aisne with this relationship is also rather good except for predictions of distances corresponding to large flow events (Fig. 8). This results in an underestimation of the distance, probably because of the different resolutions in the hydrological data. The Aisne instantaneous discharge

522 data (used to calculate the SI) are indeed measured every hour whereas the Morvan data are measured
523 every 15 minutes. It is then possible that the highest peak discharges, and consequently the maximum
524 excess stream powers were less precisely recorded for the Aisne river.

525 **5.3 The dominant influence of relative grain size: meanings and trails to explore**

526 Our study supports the idea that bed sorting and grain size range distribution greatly affect sediment
527 transport. The site with the lowest mobility (S3) is also the site with the poorest bed sorting (Table 1).
528 Previous studies indicate that a low relative grain size can increase the critical threshold for sediment
529 mobilization (Mao *et al.,* 2008; Gob *et al.*, 2010; Parker *et al.,* 2011). Our work shows that it may also
530 affect bedload transport by limiting the travel distance. This effect may be seen as the result of higher
531 critical conditions: (i) for sediment entrainment, delaying sediment departure; (ii) for sediment transport
532 itself, with coarse grains that stand in the way or increase flow resistance, then reducing sediment step
533 length.

534 The dominant influence of relative grain size on bedload tracer distances may have implications on the
535 type of bedload mobility occurring in Morvan rivers. Indeed, the hidden / exposure effect due to relative
536 grain size is likely to foster selective mobility and even an equal mobility in the stream beds where
537 sediment motion is the most determined by relative grain size (Robert, 1993, 2003; Wohl, 2014). Equal
538 mobility due to the presence of large particles on the bed has been notably underlined by Klösch and
539 Habersack (2018) on the Puerto Rican Mameyes river (data from Phillips *et al.,* 2013), which has a
540 similar morphology to the Morvan rivers. The low bedload tracer distances on the S3 site could then
541 come from the quasi absence of movement of coarse particles that hide the smaller ones and foster the
542 formation of pebble clusters and other imbricated structures. The question of the current competence of
543 the river and its ability to entrain these very coarse grains is therefore essential for the general mobility
544 of all gravel fractions.

545 Conditions around equal mobility is all the more likely to occur when there is a deficit of the medium
546 grain size fraction and a more or less well-formed armored layer (Parker and Klingeman, 1982). On the
547 S3 Cure site, one may notice a highly stable interlocked configuration around large grains but not really

548 the mobile armor in the surface layer that is often associated with equal mobility (Parker and Klingeman,
549 1982). In fact, the bed of the Cure on the S3 reach corresponds to a static armor (Sutherland, 1987;
550 Parker and Sutherland, 1990). This is also why conditions of equal mobility are partial on the S3 Cure
551 site: critical conditions for erosion and transport, and entrainment resistance are heightened for medium
552 and small grain size fractions (low relative grain size, and potential imbrication) but they seem to remain
553 very high for coarse, apparently immobile, cobbles and boulders.

554 Big particles are also present on the S7 Yonne river site but they lay among a considerable amount of
555 medium grain size fractions (see sorting index in Table 1). This lower heterogeneity of the substrate and
556 the lower relative grain size explain the differences of mean distances regarding S3, especially with
557 stream impulse values and slope that are comparable and quite close on both sites. In the S7 morpho-
558 sedimentary configuration, the sheltering effect of coarse cobbles and boulders also exists but influences
559 the displacement of smaller particles to a lesser degree.

560 The dominant influence of the relative grain size on bedload distances underlines the influence of micro
561 bed topography, especially in plane-bed rivers with heterogeneous grain size distribution. Indeed, in the
562 absence of medium or large-scale bedforms consuming the river's' energy (meanders, alluvial bars, step-
563 pool or riffle-pool sequences, etc.) (Petit *et al.* 2005), the role of the surrounding particles in the
564 entrainment resistance of a given particle (sheltering / protrusion effect) is all the more important. This
565 also invites us to examine more deeply the influence on bedload distances of small-scale characteristics
566 other than relative grain size, such as imbrication degree, micro-scale bed forms (e.g. pebble clusters)
567 and grain scale flow resistance (Robert, 1990; 2003; Lamb *et al*., 2017) in the context of plane-bed
568 morphology.

569 **5.4 The complex influence of the slope on bedload mean distances**

570 The bed slope is the second most significant parameter influencing mean bedload distance according to
571 our multivariate analysis. The first reason is of course that slope conditions the energy of the river. The
572 second reason is less obvious, it is because slope may increase flow resistance by favoring a low relative
573 flow depth (Bathurst, 2002; Lamb *et al*., 2008; Parker *et al.*, 2011; Lamb *et al*., 2017). This leads to a

574 decrease of the transport rate and/or an increase in critical conditions (Miyuzama, 1977; Shvidchenko
575 and Pender, 2000; Mao *et al.* 2008; Chiari *et al.,* 2010; Parker *et al.* 2011; Prancevic and Lamb, 2015;
576 Bunte *et al*., 2013; Lamb *et al.*, 2017). A low relative flow depth may also lower transport activity by
577 reducing the intensity of turbulent fluctuations (Sumer *et al*., 2003; Lamb *et al.,* 2017). All these
578 elements are partly supported by our study in which bedload distances appear positively correlated to
579 relative flow depth (Fig. 7C). However, from our multivariate analysis it emerged the relative flow depth
580 was an insignificant explanatory variable despite its evident link with the slope.

581 For the S5 and S3 study sites, slope appears to be negatively correlated to bedload distances. S3 has the
582 highest bed slope (with S7) but the shortest mean distance (for comparable SI) (Tables 1 and 3; Fig. 6).
583 On the other hand, S5 distances are in the high range of intermediary distances while having the lowest
584 slope (Tables 1 and 3; Fig. 6). Several studies already emphasized the positive relationship between
585 slope and critical shear stress (Mizuyama, 1977; Mueller *et al.,* 2005; Lamb *et al.,* 2008; Gob *et al.* 2010;
586 Parker *et al.*, 2011). The negative correlation between slope and bedload distances we observe on several
587 of our sites is therefore not totally unexpected. Slope may lower bedload distances when its effect is
588 dominated by an increased flow resistance and energy loss. As for relative grain size, these "negative
589 effects" of slope may diminish bedload distances in two ways: they may heighten critical conditions for
590 sediment entrainment and then delay their incipient motion for a flood event or reduce the frequency of
591 mobilization; they may also lead the mobilized particles to settle faster and then reduce the displacement
592 length.

593 Among the three sites with the steepest slopes (S3, S7, S8), two (S7 and S8) have logically the longest
594 mean distances (for a comparable SI) (Table 1 and 3; Fig. 6). They also have a higher relative depth and
595 relative grain size compared to S3. This is also true for the three remaining sites (S2, S5 and S6) with a
596 lower slope and lower intermediary mean distances. In line with S2, S6, S7 and S8 data, travel distance
597 tends to increase with channel slope. These observations suggest that slope acts positively on bedload
598 transport as long as relative depth and relative grain size remain above a certain threshold (in our case
599 ≈ 2.5 and 0.50 respectively).

600 The S5 Chalaux site differs slightly from this trend: globally it presents comparable or higher distances
601 than the S2 Cure site and the S6 Yonne site, with the highest relative depth and relative grain size, but
602 with the lowest slope (Table 1 and 3; Fig. 6). It is also the site with the lowest w/d ratio, even if the direct
603 influence of this parameter on bedload transport was not recognized as significant. These elements imply
604 that the impact of slope on transport may be a function of its combination with other parameters such as
605 flow depth, determined by discharge, flow velocity and river geometry, grain size distribution of the
606 river bed, *etc.* It may also suggest that if slope may heighten critical conditions for sediment entrainment
607 (Mizuyama, 1977; Lamb *et al.,* 2008; Gob *et al.* 2010; Parker *et al.*, 2011), in some situations (S7 and
608 S8), it may increase sediment displacement length once particles are put in motion. The seemingly
609 ambivalent role of slope on Morvan rivers calls to mind the observation of Prancevic and Lamb (2015)
610 of the absence of a universal trend in the relationship between critical dimensionless shear stress and
611 channel slope.

612 **5.5 Validity of the model equation and methodological choices**

613 The different results presented in this paper have been, for the most part, statistically valid and the model
614 equation (Eq. (4)) obtained from the multiple linear regressions have been convincingly validated by the
615 independent data set of the Aisne river. The margin of error associated with bedload displacement (0.6
616 to 1m, due to the precision of the RFID Antenna and the precision of our methodology to survey the
617 tagged particles) may be considered as quite low. Indeed, mean travel distance per inter-survey period
618 is 16.3 m (immobile tracers included). The error associated with the marked particle location represents
619 therefore only 4 to 6 % of the distance travelled.

620 Several choices that have been made in this paper could have led to uncertainties that may call into
621 question our results and, therefore, require further discussion.

622 The first of these choices concerns the threshold for sediment incipient motion. Unfortunately, it was
623 not possible to determine this precisely from our RFID surveys. Yet the critical discharge is a key
624 parameter for the calculation of stream impulse or excess stream power. Our choice to consider a
625 threshold that equals $0.7*Q_{bf}$ is therefore a strong assumption that has been widely discussed in the

methods section. In the end, our results show that our choice was probably quite accurate, especially since Eq. (4) has provided very good estimations of travel distance for the independent data of the Aisne river, for which the incipient motion threshold has been determined empirically on the field. Having said that, further investigations on the exact critical discharge would be worthwhile.

The second of our methodological choices that could have led to a certain level of uncertainty concerns the size of the largest particles tagged. Indeed, because of our tagging protocol, the coarsest particles of the riverbed (> 175 mm) were not tagged. This may have induced an underestimation of the maximum competence of the river. However, we think that these large cobbles and blocks that have not been marked are in fact immobile. Firstly, the largest particles we tagged did not moved or barely moved (Table 3 and Fig. 4). Secondly, several indications such as moss, black biofilm, stable imbrication, *etc*. show that the largest cobbles and the boulders present in the bed should not be considered as bedload under the current hydrological conditions.

6. Conclusions

The bedload transport of Morvan rivers is complex and depends on a range of parameters. The multi-peak characteristic of our surveys requires the integration of every discharge over the critical threshold, in terms of intensity and duration, and not only the highest peak, in order to evaluate the hydrological influence on bedload travel distances. The time integrated energy parameter we use – stream impulse – enables us to give more meaning to our data. However, it is not sufficient to fully understand the recorded differences of bedload displacements as the dispersion of tracer distances draws three distinct relationships. Also, when plotted with a classical energy indicator (excess specific stream power), bedload displacements cover a wide range of values obtained from other studies on different channel morphological types (plane-bed, riffle-pool, step-pool). This variability of distance values leads us to investigate the influence of more specific morphological and hydraulic parameters (and the role of their own variability) on bedload transport in a plane-bed context. The stream impulse and the other four hydro-morphometric parameters that we tested (relative grain size, relative flow depth, slope, w/d ratio) bring us useful information to highlight what controls bedload transport on Morvan rivers. The multiple

regression analysis indicates that the relative grain size, the slope and the stream impulse are, in order of significance, the most important parameters influencing bedload distances.

Relative grain size, the first controlling factor on bedload mean distance on Morvan rivers, emphasizes the importance of microtopography and grain size distribution range in plane-bed rivers. Substrate arrangement and very coarse particles compose various grain/micro to medium scale features. These are probably even more important to consider in this plane-bed channel morphology as they represent the main constraints to particle entrainment (hiding effect, imbrication, stable sedimentary structures) and the main sources of flow resistance (immobile cobbles and boulders, transverse ribs, clusters).

The role of the slope has already been studied in relation to critical conditions for incipient motion. Our study shows that it significantly affects direct bedload distances. The way in which bed slope has an influence is ambiguous though, and seems to depend on other hydro-morphometric factors: it notably appears to act in favor of bedload travel distances when the coarsest particles are largely submerged ($d/D_{84} > 2.5$ at least). Nonetheless, the multiple regression suggests that slope impacts bedload distances more significantly in other ways.

The single model equation we obtained to predict mean bedload distance (Eq. (4)), combining stream impulse (SI), relative grain size and bed slope, functions pretty well with our own data and with data from the Aisne river. However, it is wise to pursue these validation tests further, with other data that are equivalent to ours (data collection method, geomorphological settings). If validity is confirmed, tests with other morphological types of fluvial systems and in different morpho-climatic contexts will be needed to determine the application range of the model.

Acknowledgments

The authors would like to thank Matthieu Moës and the Agence de l'Eau Seine-Normandie (public water agency), for financing the research work leading to this paper. We are also very grateful to Jean-René Malavoi and Electricity de France (EDF) as well as the PIREN Seine for the financial support they provided for the purchase of research equipment and for fieldwork missions. We extend our sincere appreciation to Jonathan Touche for his help on the field and Natasha Shields for her assistance in

translating. Finally, we would like to thank F. Comiti and the anonymous reviewer for their thoughtful comments that enabled the quality of the original paper to be greatly improved.

References

Andrews, E.D., Nankervis, J.M., 1995. Effective Discharge and the Design of Channel Maintenance Flows for Gravel-Bed Rivers. Geophysical Monograph Series 89, 151-164.

Arnaud, F. Piégay., H., Vaudor, L., Bultingaire, L., Fantino, G., 2015. Technical specifications of low-frequency radio identification bedload tracking from field experiments: Differences in antennas, tags and operators. Geomorphology 238, 37–46.

Arnaud, F., Piégay, H., Béal, D., Collery, P., Vaudor, L., Rollet, A.J., 2017. Monitoring gravel augmentation in a large regulated river and implications for process-based restoration. Earth Surface Processes and Landforms 42 (13), 2147–2166.

Assani, A.A., Petit, F., 2004. Impact of hydroelectric power releases on the morphology and sedimentology of the bed of the Warche river (Belgium). Earth Surface Processes and Landforms 29, 133-143.

Bagnold, RA., 1980. An empirical correlation of bedload transport rates in flumes and natural rivers. Proceedings of the Royal Society of London A 372, 453–473.

Bathurst, J.C., 2002. At-a-site variation and minimum flow resistance for mountain rivers. Journal of Hydrology 269, 11–26.

Belliard, J., Albert, M.B., Gob, F., Sauquet, E., Catalogne, C., Zahm, A. 2009. Caractérisation des altérations physiques et de leurs conséquences écologiques des rivières du bassin Seine-Normandie. Phase I: cas des cours d'eau de la Craie. Accord-cadre Agence de l'Eau Seine Normandie (AESN)/Cemagref., 85 p

Bradley, N., Tucker, G.E., 2012. Measuring gravel transport and dispersion in a mountain river using passive radio tracers. Earth Surface Processes and Landforms, 37, 1034–1045.

Bravard, J.P., Petit, F., 1997. Les cours d'eau, Dynamique du système fluvial. Armand Colin, Paris, 222 pp.

Bright, C.J., 2014. Development of an RFID approach to monitoring bedload sediment transport and a field case study. Ph.D thesis, University of Waterloo, 255 pp.

Bunte, K., Abt, S. R., Swingle, K. W., Cenderelli, D. A., and Schneider, J. M.,2013. Critical Shields values in coarse bedded steep streams, Water Resources Research, 49, 7427– 7447.

Chapuis, M., Bright, C.J., Hufnagel, J., MacVicar, B., 2014. Detection ranges and uncertainty of passive Radio Frequency Identification (RFID) transponders for sediment tracking in gravel rivers and coastal environments. Earth Surface Processes and Landforms 39, 2109–2120.

Chiari, M., Friedl, K., Rickenmann, D. 2010. A one-dimensional bedload transport model for steep slopes, Journal of Hydraulic Research, 48:2, 152-160.

Church, M., Hassan, M.A., 1992. Size and distance of travel of unconstrained clasts on a streambed. Water Resources Research 28, 299–303.

718 Dell'Agnese, A., Brardinoni, F., Toro, M., Mao, L., Engel, M., Comiti, F., 2015. Bedload transport in a
719 formerly glaciated mountain catchment constrained by particle tracking. Earth Surface Dynamics, 3,
720 527-542.

721 Dépret T., Riquier R., Piégay H., 2017. Evolution of abandoned channels: Insights on controlling factors
722 in a multi-pressure river system. Geomorphology, 294, 99-118.

723 Ferguson, R., Wathen, S., 1998. Tracer-pebble movement along a concave river profile: virtual velocity
724 in relation to grain size and shear stress. Water Resources Research 34, 2031–2038.

725 Ferguson, R.I., Bloomer, D.J., Hoey, T.B.,Werritty, A., 2002. Mobility of river tracer pebbles over
726 different timescales. Water Resource Research 38 (5, 1045), 3-1-3-8.

727 Ferguson, R., Hoey, T., 2002. Long-term slowdown of river tracer pebbles: generic models and
728 implications for interpreting short-term tracer studies. Water Resources Research 38 (8, 1142), 17-1-17-
729 11.

730 Gilet, L., Gob, F., Virmoux, C., Touche, J., Harrache, S., Gautier, E., Moës, M., Thommeret, N., Jacob-
731 Rousseau N., 2018. Suivi de l'évolution morphologique et sédimentaire de l'Yonne suite à la première
732 phase du démantèlement du barrage de Pierre Glissotte (Massif du Morvan, France). Géomorphologie :
733 relief, processus, environnement, 24 (1), 7-29.

734 Gintz, D., Hassan, MA., Schmidt, K.H., 1996. Frequency and magnitude of bedload transport in a
735 mountain river. Earth Surface Processes and Landforms, 21, 433–445.

736 Gob, F., Bravard, J.P., Petit, F., 2010. The influence of sediment size, relative grain size and channel
737 slope on initiation of sediment motion in boulder bed rivers. A lichenometric study. Earth Surface
738 Processes and Landforms, 35, 1535-1547.

739 Haschenburger, J.K., 2011. The rate of fluvial gravel dispersion. Geophysical research letters 38,
740 (L24403).
741
742 Haschenburger, J.K, 2013. Tracing river gravels: insights into dispersion from a long-term field
743 experiment. Geomorphology 200, 121–131.
744
745 Haschenburger, J.K., Church, M., 1998. Bed material transport estimated from the virtual velocity of
746 sediment. Earth Surface Processes and Landforms 23, 791–808.
747
748 Hassan, M.A., Church, M., Schick A.P., 1991. Distance of movement of coarse particles in gravel bed
749 streams. Water Resources Research, 27, 503–511.
750
751 Hassan, M.A., Church, M., 1992. The movement of individual grains on the streambed. In:
752 Billi, P., Hey, R.D., Thorne, C.R., Tacconi, P. (Eds.), Dynamics of Gravel-Bed Rivers.
753 Wiley, New-York, pp. 159–175.
754
755 Hassan, M.A., Church, M., Ashworth, P.J., 1992. Virtual rate and mean distance of travel of
756 individual clasts in gravel-bed channels. Earth Surface Processes and Landforms, 17, 617–627.
757
758 Hassan, M., Bradley, D.N., 2017. Geomorphic controls on tracer particle dispersion in gravel bed rivers.
759 In: Tsutsumi, D., Laronne, J.B. (Eds), Gravel-Bed Rivers, Processes and Disasters,.Wiley-Blackwell,
760 UK, pp. 439–466.
761
762 Houbrechts, G., Hallot, E., Gob, F., Mols, J., Defechereux, O., Petit, F., 2006. Frequency and extent of
763 bedload transport in rivers of the Ardenne. Géographie Physique et Quaternaire 60 (3), 247-258.
764 Houbrechts, G., Campenhout, J.V., Levecq, Y., Hallot, E., Peeters, A., Petit, F., 2012. Comparison of
765 methods for quantifying active layer dynamics and bedload discharge in armoured gravel-bed rivers.
766 Earth Surface Processes and Landforms 37, 1501-1517.

Houbrechts, G., Levecq, Y., Peeters, A., Hallot, E., Campenhout, J.V., Denis, A.C., Petit, F. (2015) – Evaluation of long-term bedload virtual velocity in gravel-bed rivers (Ardenne, Belgium). Geomorphology 251, 6-19.

Jaeggi, M.N.R., 1987. Interaction of bed load transport with bars. In: Thorne, C.R., Bathurst, J.C., Hey, R.D. (Eds.), Sediment Transport in Gravel-Bed Rivers.Wiley, Chichester, UK, pp. 829–841.

Klösch, M., Habersack, H., 2018. Deriving formulas for an unsteady virtual velocity of bedload tracers. Earth Surface Processes and Landforms 43, 1529-1541.

Lamarre, H., Roy, A.G., MacVicar, B., 2005. Using PIT tags to investigate sediment transport in gravel-bed rivers. Journal of Sedimentary Research 75 (4), 736-741.

Lamarre, H., Roy, A.G., 2008. The role of morphology on the displacement of particles in a step–pool river system. Geomorphology 99, 270–279.

Lamb, M.P., Dietrich, W.E., Venditti, J.G., 2008. Is the critical Shields stress for incipient sediment motion dependent on channel-bed slope? Journal of Geophysical Research-Earth Surface 113 (F02008).

Lamb, M.P., Brun, F., Fuller, B.M., 2017. Direct measurements of lift and drag on shallowly submerged cobbles in steep streams: Implications for flow resistance and sediment transport. Water Resource Research 53 (9), 7607-7629.

Laronne, J.B, Outhet, D.N., Duckman, J.L., 1992. Determining event bedload volume for evaluation of potential degradation sites due to gravel extraction, N.S.W., Australia. In: Erosion and Sediment Transport Monitoring Programmes in River Basins (Proceedings of the Oslo Symposium, August 1992), IAHS Publications 210. IAHS Press, Wallingford, 87–94

Lenzi, M.A, 2004. Displacement and transport of marked pebbles, cobbles and boulders during floods in a steep mountain stream. Hydrological Processes, 18, 1899–1914.

Lejot, J. 2008. Suivi des formes fluviales par télédétection à très haute résolution. Application aux programmes de restauration de la basse vallée de l'Ain et du Haut-Rhône (Chautagne). Thèse de doctorat, Université Lumière Lyon 2, 257p.

Liébault, F., Clément, P., 2007. La mobilité de la charge de fond des rivières torrentielles méditerranéennes. Géographie Physique et Quaternaire 61 (1), 7–20.

Liébault, F., Laronne, J.B., 2008. Evaluation of bedload yield in gravel-bed rivers using scour chains and painted tracers: the case of the Esconavette Torrent (southern French Prealps). Geodinamica Acta 21, 23–34.

Liébault, F., Bellot, H., Chapuis, M., Klotz, S., Deschâtres, M., 2012. Bedload tracing in a high-sediment-load mountain stream. Earth Surface Processes and Landforms, 37, 385-399.

Madej, M. A., Ozaki,V., 1996. Channel response to sediment wave propagation and movement, Redwood Creek, California, USA. Earth Surface Processes Landforms 21, 911–927.

Mao, L., Uyttendaele, G.A., Iroumé, A., Lenzi, M.A. 2008. Field based analysis of sediment entrainment in two high gradient streams located in Alpine and Andine environ-ments. Geomorphology 93, 368–383.

Mao, L., Picco, P., Lenzi, M.A., Surian, N., 2017a. Bed material transport estimate in large gravel-bed rivers using the virtual velocity approach. Earth Surface Processes and Landforms, 42, 595-611.

816 Mao, L., Dell'Agnese, A., Comiti, F. 2017b. Sediment motion and velocity in a glacier-fed stream.
817 Geomorphology, 291, 69-79.

818 Métivier, F., Lajeunesse, E., Devauchelle, O., 2017. Laboratory rivers: Lacey's law, threshold theory,
819 and channel stability. Earth Surface Dynamics 5, 187–198.

820 Milan, D.J., 2013. Virtual velocity of tracers in a gravel-bed river using size-based competence duration.
821 Geomorphology 198, 107–114.

822 Mizuyama, T., 1977. Bedload transport in steep channels. Ph.D thesis, University of Kyoto, 123 pp.

823 Moog, D.B., Whiting, P.J., 1998. Annual hysteresis in bed load rating curves. Water Resources Research
824 34 (9), 2393-2399.

825 Mueller, E.R., Pitlick, J., Nelson, J.M., 2005. Variation in the reference Shields stress for bed load
826 transport in gravel-bed streams and rivers. Water resources research 41(4), 1–10.

827 Olinde, L., Johnson, J.P.L., 2015. Using RFID and accelerometer-embedded tracers to measure
828 probabilities of bed load transport, step lengths, and rest times in a mountain stream. Water Resource.
829 Research 51, 7572–7589.

830 Papangelakis, E., 2013. The effects of channel morphology on the mobility and dispersion of sediment
831 in a small gravel-bed stream. Master thesis, University of Toronto, 93 pp.

832 Papangelakis, E, Hassan, M. 2016. The role of channel morphology on the mobility and dispersion of
833 bed sediment in a small gravel-bed stream. Earth Surface Processes and Landforms 41, 2191-2206.

834 Parker, G., Klingeman, P.C., 1982. On why gravel-beds streams are paved. Water Resources Research
835 18, 1409–1423.

836 Parker, G., Sutherland, A.J., 1990. Fluvial armour. Journal of Hydraulic Research 28, 529–544.

837 Parker, C., Clifford, N.J., Thorne C.R., 2011. Understanding the influence of slope on the threshold of
838 coarse grain motion: revisiting critical stream power. Geomorphology 126, 51-65.

839 Petit, F., Gob, F., Houbrechts, G., Assani, A.A., 2005. Critical specific stream power in gravel-bed rivers.
840 Geomorphology 69 (1-4), 92-101.

841 Pfeiffer, A.M., Finnegan, N.J.,Willenbring, J.K., 2017. Sediment supply controls equilibrium channel
842 geometry in gravel rivers. PNAS, 114 (13), 3346-3351.

843 Phillips, C.B., Martin, Raleigh, L., Jerolmack, D.J., 2013. Impulse framework for unsteady flows reveals
844 superdiffusive bed load transport. Geophysical Research letters 40, 1328-1333.
845
846 Phillips, C.B, Jerolmack, D.J., 2014. Dynamics and mechanics of bed-load tracer particles. Earth Surface
847 Dynamics 2, 513-530.
848
849 Phillips, J.D., 2015. Hydrologic and geomorphic flow thresholds in the Lower Brazos River, Texas,
850 USA, Hydrological Sciences Journal 60,9, 1631-1647.
851
852 Pitlick, J., Cress, R., 2000. Longitudinal trends in channel characteristics of the Colorado River and
853 implications for food-web dynamics. Final report to the recovery program for the endangered fishes of
854 the upper Colorado River, project number 48, department of geography, University of Colorado, 52 pp.
855
856 Piégay, H., Arnaud, F., Cassel, M., Dépret, T., Alber, A., Michel, K., Rollet A.J., Vaudor, L.**,** 2016. Suivi
857 par RFID de la mobilité des galets : retour sur 10 ans d'expérience en grandes rivières. Bulletin de la
858 Société Géographique de Liège 67 , 77-91.
859

Prancevic, J., Lamb, M.P., 2015. Unraveling bed slope from relative roughness in initial sediment motion. Journal of Geophysical Research: Earth Surface 120 (3), 474–489.

Pyrce, R.S., Ashmore, P.E., 2003a. The relation between particle path length distributions and channel morphology in gravel-bed streams: a synthesis. Geomorphology 56, 167–187.

Pyrce, R.S., Ashmore, P.E., 2003b. Particle path length distributions in meandering gravel-bed streams: results from physical models. Earth Surface Processes and Landforms 28(9), 951–966.

Pyrce, R.S., Ashmore, P.E., 2005. Bedload path length and point bar development in gravel-bed river models. Sedimentology 52, 839–857.

Robert, A., 1990. Boundary roughness in coarse-grained channels. Progress in Physical Geography: Earth and Environment 14, 42–70.

Robert, A., 1993. Bed configuration and microscale processes in alluvial channels. Progress in Physical Geography 17 (2), 123-136.

Robert, 2003. A. River Processes. Hodder Education, London, 214 pp.

Rollet A.J., Macvicar B., Piégay H., Roy A., 2008. Utilisation de transpondeurs passifs pour l'estimation du transport sédimentaire : premiers retours d'expérience. La Houille Blanche - Revue internationale de l'eau, EDP Sciences, 2008.

Scheingross, J.S., Winchell, E.W., Lamb, M.P., Dietrich, W.E., 2013. Influence of bed patchiness, slope, grain hiding, and form drag on gravel mobilization in very steep streams, Journal of Geophysical Research: Earth Surface, 118, 982–1001Schneider, J., Turowski, J., Rickenmann, D., Hegglin, R., Arrigo, S., Mao, L., Kirchner, J., 2014. Scaling relationships between bed load volumes, transport distances, and stream power in steep mountain channels, Journal of Geophysical Research : Earth Surface 119 (3), 533–549.

Shvidchenko, A.B., Pender, G., 2000. Flume study of the effect of relative depth on the incipient motion of coarse uniform sediments. Water Resources Research 36(2), 619-628.

Sumer, B. M., L. H. C. Chua, N. S. Cheng, and J. Fredsoe. 2003. Influence of turbulence on bed load sediment transport, J. Hydraul. Eng., 129 585– 595.

Sutherland, A.J., 1987. Static armor layers by selective erosion. In: Thorne, C.R, Bathurst, J.C, Hey, R.D (Eds), Sediment transport in gravel-bed Rivers. Wiley, Chichester, 243–267

Sutherland, D.G., Hansler Ball, M., Hilton, S.J., Lisle, T.E., 2002. Evolution of a landslide induced sediment wave in the Navarro River, California. Geological Society of America Bulletin 114 (8), 1036–1048.

Wilcock P.R., 1997. Entrainment, displacement, and transport of tracer gravels. Earth Surface Processes and Landforms 22, 1125–1138.

Wohl, E., 2014. Rivers in the landscape. Wiley-Blackwell, UK, 330 pp.

Wolman, M.G., 1954. A method of sampling coarse bed material. American Geophysical Union Transactions 35, 951–956.